Comprehensive investigations of ablative plasma and crater formation in experiments at PALS related to Shock Ignition concept

T. Pisarczyk[1], S.Yu. Gus'kov[2,3], O. Renner[4], N.N. Demchenko[2], M. Smid[4], R. Dudzak[6,4], T. Chodukowski[1], Kalinowska[1], M. Rosinski[1], P. Parys[1], J. Dostal[6,4] J. Badziak[1], D. Batani[5], S. Borodziuk[1], E. Krousky[6,4], L. Antonelli[5], Y. Maheut[5], G. Cristoforetti[7], L.A. Gizzi[7], P. Koester[7], L. Labate[7], F. Baffigi, J. Ullschmied[6,4], J. Hrebicek[4,6], T. Medrik[4,6], M. Pfeifer[6,4], J. Skala[6,4], P. Pisarczyk[7]

[1] Institute of Plasma Physics and Laser Microfusion, Warsaw, Poland
[2] P.N. Lebedev Physical Institute of RAS, Moscow, Russian Federation
[3]National Research Nuclear University (Moscow Eng. Phys. Inst.), Russian Federation
[4] Institute of Physics ASCR, Prague, Czech Republic
[5] Université Bordeaux, CNRS, CEA, CELIA, Talence, France
[6] Institute of Plasma Physics ASCR, Prague, Czech Republic
[7]Intense Laser Irradiation Laboratory, INO-CNR, Pisa, Italy
[8] Warsaw University of Technology, ICS, Warsaw, Poland

The shock ignition (SI) is a subject dominating in the last investigations carried out at PALS facility in the frame of international cooperation within the LaserLab projects [1-5]. In the experiments two-layer targets were used, consisting of massive planar Cu coated with a thin polyethylene layer, that in the case of two-beam irradiation geometry simulate conditions related to the SI concept, namely: one of the beams (1ω or 3ω) with a high intensity $>10^{15}$ W/cm^2 generates igniting shock wave, while the other one (1ω) with the lower intensity below 10^{14} W/cm^2 creates a pre-plasma simulating pre-compressed plasma in a real inertial fusion experiment. The experiments concern the influence of the pre-plasma on efficiency of the laser radiation energy transport to a shock wave in which mechanisms of fast electron generation play an important role. This research was based on application of the multi-frame interferometry and a unique set of x-ray and ion diagnostics. In the last studies carried out with the 1ω main beam, femtosecond interferometry turned out to be especially useful [5]. It enabled to determine the changes of the electron density gradients during the laser pulse interaction with a target, which definitively confirmed an occurrence of the resonant absorption in the case of the first harmonic and its influence on the laser radiation energy transport to a shock wave. The investigations presented in this paper are related to the use of 3ω beam to create the igniting shock wave. The desired intensity of the main beam was achieved at constant laser energy on the level of 200 J by changing the focal spot radius of the laser beam on the target in the range of R_L = 50-200 μm. The pre-plasma was created by means of the 1ω laser radiation with the energy of 40 J which was defocused to the focal spot radius of R_L = 300 μm. In the experiments, two-layer targets were used consisting of a planar massive Cu covered by thin layer of polyethylene with different thicknesses. Analogously as in studies [5], the following diagnostics were used: the 3-frame interferometer irradiated by a femtosecond Ti: Sa laser (t = 40 fs and λ = 808 nm), 2D imaging of the Cu K_α emission to determine the distribution of the fast electrons population and their energy, and the grid collectors to measure the angular distributions of the ion emission. As the routine diagnostic, the crater volume measurements were carried to evaluate the efficiency of the laser energy transfer to the shock wave generated in the massive part of the two-layer targets.

The femtosecond interferometry was applied to determine the electron density distributions in ablative plasma during the laser beam interaction with the target at different irradiation conditions in the case of absence and presence of the pre-plasma. The obtained electron density distributions prove that the light plasma with the higher pressure generated from the

thin plastic layer by an auxiliary beam limits the radial expansion of the central plasma created by the 3ω main laser beam. The radial constrain favours the axial character of the plasma expansion particularly in the case of larger R_L. On the basis of the space time density distributions, the information about the maximal density gradients, the scalelength (L) and the total electron number (N) in the ablative plasma were determined. To obtain the information about the density scalelength, an exponential fitting of the axial density profiles has been applied: $n_e(z) = n_0 e^{-z/L}$. The changes of the axial density profiles and the L caused by increasing R_L in the case with and without the pre-plasma are demonstrated in Fig. 1a, while in Fig 1b the dependences of the maximal gradient density are shown.

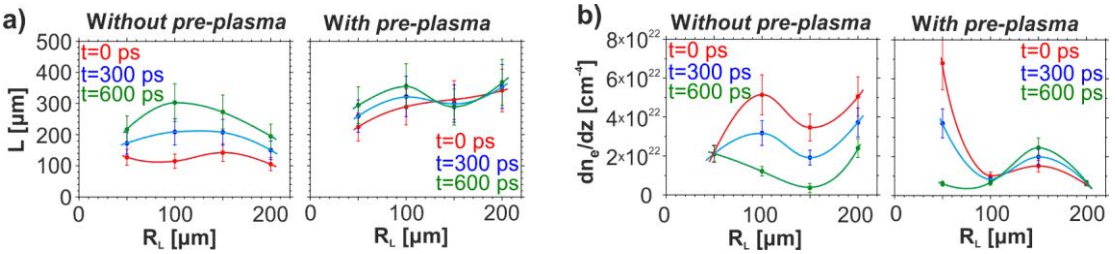

Fig. 1. The changes of L - a) and N-b) as a function of R_L for different expansion times in the case of the absence and the presence of the pre-plasma.

These dependences prove that in the case without the pre-plasma, the non-collisional processes with the L ≅100 μm can develop in the whole range of the varied R_L (such as the resonance absorption). The pre-plasma causes significant extension of L (about 3 times) and creates conditions for the development of the processes with the large-scale gradient that simultaneously require high electron density. This suggests two maxima relating to both the density and its gradient which correspond to the focal spot radii R_L = 50 and 150 μm.

Crater volume measurements combined with the interferometric investigations, allowed to obtain the N/V_{cr} parameter (where V_{cr} is the crater volume) which defines a number of thermal electrons participating in a creation of the crater volume unit (1 cm^3). The N/V_{cr} parameter was evaluated only for expansion time t= 600 ps, i.e., after the end of the main laser pulse, when both ablation process and processes related to absorption of the laser radiation were completed, Fig. 2.

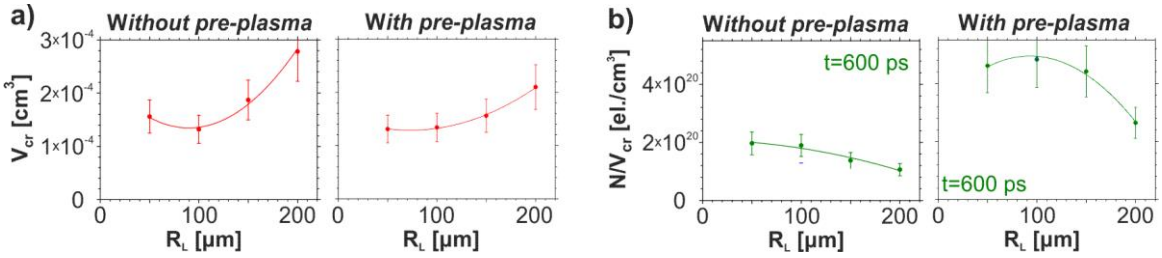

Fig. 2 The changes of V_{cr}-a) and N/V_{cr}-b) parameter caused by the increasing R_L and by the pre-plasma presence.

In the case without pre-plasma, increase in V_{cr} and decrease in N/V_{cr} with the increasing R_L testifies about dominance of the collision absorption mechanism (inverse bremasstrahlung, IB) in the whole range of R_L, when the laser energy transfer to the target is achieved through the electron-thermal conductivity wave (ETC) [1, 3, 5]. For such mechanism and the 3ω laser beam the ablative pressure depends on the 1D geometry of the plasma expansion, which grows with R_L. The presence of the pre-plasma does not change the character of V_{cr} and N/V_{cr} dependences, what confirms the presence of the IB absorption and the ETC mechanism. However, the strong decrease in the N/Vcr parameter in the range of R_L=150-200 μm due to the more 1D (planar) expansion creates more favourable conditions for the crater creation.

2D imaging of the Cu K_α line emission was carried out to investigate the 1D plasma expansion occurring for the 3ω laser radiation due to the fast electron generation under

presence and absence of the pre-plasma. The imaging setup was the same as in the previous experiments [5]. To determine the energy of the fast electrons, two-layer targets with different thicknesses of the plastic (Δ_{pl} = 15, 25, 50 and 100 μm) have been used. Results mapping the Kα emission due to fast electron action are presented in Fig. 3. To determine

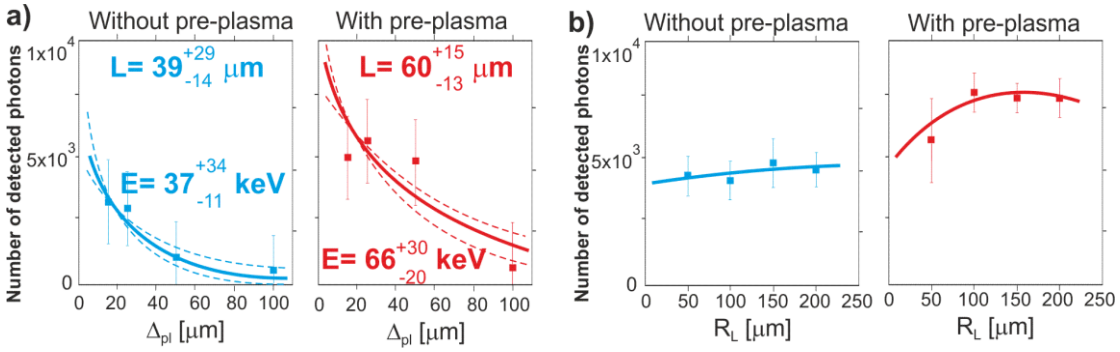

Fig. 3 Measurements of the Cu Kα emission due to generation of fast electrons demonstrate the influence of the pre-plasma on the total population of photons in dependence on: a) Δ_{pl} and b) R_L

the energy of fast electrons, an exponential decay of the photon emission with the increasing thickness of the plastic layer I (x) = A * exp (-x / L) was assumed. It was fitted to the experimental data using a Monte Carlo method assuming Maxwellian distribution of the suprathermal electron energy and electron impact on the double layer target [6]. Calculations showed that the average energy of fast electrons in the case of no pre-plasma), is about 37 keV, i.e., almost two times smaller than in the case of the pre-plasma presence, Fig. 3a. The presence of pre-plasma, Fig. 3b, significantly increases the emission of fast electrons with the increasing R_L. Therefore we can conclude that the 1D expansion of the ablative plasma in the presence of the pre-plasma increases both the emission and the energy of the fast electrons, thus suggesting that besides the IB mechanism also non-collisional processes (such as the resonance absorption) associated with the laser energy transport by fast electrons can take place in the process of the laser energy transport and the pressure formation.

The ion measurements are in agreement with the interferometry and confirm the limited radial expansion of the central plasma created by means of the 3ω main laser beam due to lower-Z plasma with the higher pressure generated from the thin plastic layer by auxiliary beam.

2D numerical simulations were carried out using the 2D hydrodynamic code ATLANT-HE [7] which includes modelling of the laser radiation refraction in the plasma, inverse bremsstrahlung and resonance absorption of the laser radiation, generation of fast electrons due to the resonance absorption, and the fast electron energy transfer with Coulomb collisions. The calculations were made for conditions of the experiment. A satisfactory agreement of calculations with the experiment was obtained in the case of the laser beam interaction with the target in the presence of the pre-plasma, as illustrated by the data in the Table 1 and 2. In the case of the pre-plasma absence, the qualitative character is the same but the observed and simulated L values differ considerably. The large values of experimental L result from the action of the temporally extended beam profile which is characteristic for the PALS laser and contributes to the creation of the low density plasma even in the case of the pre-pulse absence. In Table 2 the numerical simulations of the total (δ_{total}), the resonant (δ_{res}) and the inverse bremsstrahlung δ_{ib} absorption coefficients are compared for the cases of the pre-plasma absence and presence. It should be noted that in the presence of the pre-plasma, the fast electron energy is close to the experimental values, obtained from Cu K_α line measurements. Table 2 clearly indicates that in the case of the absence of the pre-plasma, the total absorption increases with the increasing focal spot radius from the value 0.593 to 0.876.

In contrast, the fraction of resonant absorption decreases from 0.0883 to 0.0697 and stays small. The average energy of fast electrons $E_{h(max)}/2$ is about 30-35 keV for both with and without pre-plasma cases.. Pre-pulse has a small effect on these quantities and does not alter their dependence on the radius of the main beam. These results differ significantly from the case of the 1ω main pulse which was presented in [5].

Table 1

L [μm]				
	3ω		1ω+3ω	
R_L [μm]	Exp	2D	Exp	2D
50	125	39	220	298
100	115	34	290	307
200	100	29	340	283

Table 2

R_L [μm]	50		100		200	
	3ω	1ω+3ω	3ω	1ω+3ω	3ω	1ω+3ω
δ_{total}	0.593	0.553	0.751	0.691	0.876	0.789
δ_{ib}	0.505	0.462	0.655	0.592	0.806	0.716
δ_{res}	0.0883	0.091	0.0963	0.0993	0.0697	0.0733
$E_{h(max)}$, keV	69.4	73.8	62.3	69.6	58.2	54.8
T_{emax}, keV	3.67	3.91	2.81	3.27	2.09	2.58

Conclusions: ***Interferometric studies*** of the ablative plasma expansion in combination with the crater volume measurements and the measurements of the Cu K_α emission due to fast electrons confirm the clear influence of the expansion geometry on the efficiency of the laser energy transport to the shock wave and the ablative pressure formation as well as the fast electron generation. The increase of R_L leads to an increase of both the efficiency of the laser energy transport to the target and the fast electron production. Pre-plasma does not significantly change the character of these dependencies, however it strongly influences an increase of the fast electrons energy. ***Numerical simulations*** show that without the pre-plasma, the total absorption is considerably larger for 3ω than that of the 1ω main pulse. This is confirmed by data from ion collector measurements. The fraction of the resonance absorption is about the same. Pre-plasma has a small effect on absorption in the case of the 3ω and strong effect in the case of the 1ω. In the case of the pre-plasma, for the 3ω main pulse the fraction of resonance absorption (and hence the energy contained in the fast electrons) is several times smaller than for the 1ω main pulse. This is confirmed by ion collector measurements, too. The average energy of fast electrons generated by resonant absorption is approximately two times smaller in the case of the 3ω main pulse (~30-35 keV) as compared with the 1ω main pulse (50-70 keV) [5].

Acknowledgments: This paper was supported in part by the Access to Research Infrastructure activity in the 7th Framework Program of the EU Contract No.284464, Laserlab Europe III, by the Czech Republic's Ministry of Education, Youth and Sports under PALS RI-LM 2010014 and by the ToIFE Project of the EUROfusion Consortium and by the French-Polish bilateral collaboration program POLONIUM and of the COST Action MP1208 "Developing the physics and the Scientific Community for Inertial Fusion by Russian Foundation for Basic Research (Projects No. 14-02-00010 and No. 13-02-00295). It was also supported in part by National Centre for Science (NCN), Poland, under Grant No. 2012/04/M/ST2/00452.

Reference:

1. P. Koester et al, Plasma Physics and Controlled Fusion **55,** 124045 (2013).
2. S.Yu. Gus'kov et al, Laser Particle Beams **32,** 177-915 (2014).
3. T. Pisarczyk et al, Phys. Plasmas **21**, 012708 (2014).
4. D. Batani et al, Phys. Plasmas **21**, 032710 (2014).
5. T. Pisarczyk et al Laser and Particle Beams **33**, 221-236 (2015)
6. F.Salvat, J.M.Fernandez-Varea, and J. Sempau. Penelope-2008: A Code System for Monte Carlo Simulation of Electron and Photon Transport. 2009. ISBN 978-92-64-99066-1.
7. I. G. Lebo et al, Laser Part. Beams **22**, 267–273 (2004).